Nanoscale

Accepted Manuscript

This is an *Accepted Manuscript*, which has been through the RSC Publishing peer review process and has been accepted for publication.

Accepted Manuscripts are published online shortly after acceptance, which is prior to technical editing, formatting and proof reading. This free service from RSC Publishing allows authors to make their results available to the community, in citable form, before publication of the edited article. This *Accepted Manuscript* will be replaced by the edited and formatted *Advance Article* as soon as this is available.

To cite this manuscript please use its permanent Digital Object Identifier (DOI®), which is identical for all formats of publication.

More information about *Accepted Manuscripts* can be found in the **Information for Authors**.

Please note that technical editing may introduce minor changes to the text and/or graphics contained in the manuscript submitted by the author(s) which may alter content, and that the standard **Terms & Conditions** and the **ethical guidelines** that apply to the journal are still applicable. In no event shall the RSC be held responsible for any errors or omissions in these *Accepted Manuscript* manuscripts or any consequences arising from the use of any information contained in them.

Cite this: DOI: 10.1039/c0xx00000x

www.rsc.org/xxxxxx

ARTICLE TYPE

Loading of an Anti-cancer Drug onto Graphene Oxide and Subsequent Release to DNA/RNA: A Direct Optical Detection

Raj Kumar Koninti, Abhigyan Sengupta, Krishna Gavvala, Nirmalya Ballav*, and Partha Hazra*

Received (in XXX, XXX) Xth XXXXXXXXX 20XX, Accepted Xth XXXXXXXXX 20XX

DOI: 10.1039/b000000x

Graphene oxide based molecular switching of Ellipticine (E) has been utilized to probe its efficient loading onto graphene oxide (GO) and subsequent release to intra-cellular biomolecules like DNA/RNA. The green fluorescence of E switches to blue in GO and switches back to green by polynucleotides. The intensified blue emission of the ellipticine-GO (E-GO) complex with human serum albumin (HSA), switches to bluish green upon addition of dsDNA. Electron microscopy reveals the formation of distinctive 3D assemblies involving GO and biomolecule(s) probably through non-covalent interactions and is primarily responsible for the biomolcule(s) assisted fluorescence-switching of E. To our knowledge, such morphological pattern of GO-DNA complex is very unusual, reported here the first time and could find applications in the fabrication of biomedical devices. Moreover, our approach of direct optical detection of drug loading and releasing is very cheap, appealing and will be useful for clinical trial experiments once the cytotoxicity of GO is duly taken care.

Introduction

An important concern in chemotherapy is the targeted delivery and controlled release of anticancer drugs.[1] In order to achieve this, various nano-materials are being explored that could serve the purpose of efficient drug carriers.[2-4] In a recent perspective, Ganger *et al.*, discussed the importance of nano-bio interface in view of engineering nano-materials for various biomedical applications.[5] Recently, graphene, a two-dimensional nano-material, was discovered by Geim *et al.* in 2004[6] and its derivatives, namely, graphene oxide (GO), reduced graphene oxide (RGO) are mostly considered as nano-carriers for certain anticancer drugs.[7-14] Moreover GO can be used as efficient biomolecular sensor[15, 16] as well as pH-responsive molecular switch[17]. Unlike GO, RGO cannot be efficiently dispersed in water, due to π-π stacking and hydrophobic interactions within individual layers.[18] To increase the dispersion ability of RGO in water, lysozymes[19] and other proteins[20] are used, however, such additives may act as interfering media in course of drug loading and affect other physico-chemical properties. Thus, in view of nano-carrier activity, GO is much superior to RGO, primarily because of its unique surface-functionality (presence of polar groups and π-conjugation), better water solubility and biocompatibility.[7-12] However, one should also take into account some recent reports about the cytotoxicity of GO.[21, 22] Although the drug loading and its subsequent release have been routinely monitored by usual absorption spectroscopic techniques,[23-25] intrinsic fluorescence property of the drug may prove to be very useful due to higher sensitivity of fluorescence over absorption[13, 18]. However, instead of monitoring the fluorescence intensity, it would be very simple and effective, if the drug loading onto the carrier surface and subsequent release to specific biomolecules like DNA/RNA can be directly monitored by the change in the fluorescence colour. Herein, we have explored the distinctive interaction scenario, of GO and DNA/RNA/proteins/sugars with an important anticancer drug, ellipticine (E) (Scheme 1) which is known to intercalate in DNA and inhibits the activity of DNA topoisomerase II.[26-29] Ellipticine (E) exhibits polarity dependent dual fluorescence property,[30-32] thereby, intrinsic dual fluorescence behaviour of E can be efficiently used to probe the loading and subsequent release to bio-molecules with the help of fluorescence-switching of drug, that would avoid the complexities associated with the standard techniques.

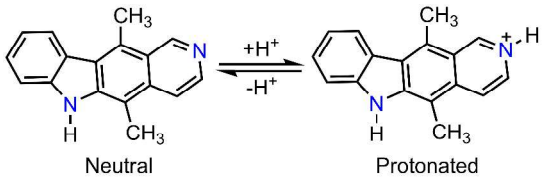

Scheme 1: Different prototropic forms of ellipticine.

The green fluorescence of ellipticine (E) in phosphate buffer solution (PBS, pH ~7) switched to blue upon addition of GO and subsequently switched back to green upon addition of either DNA or RNA. Since in reality the ellipticine-GO (E-GO) complex is supposed to travel through blood stream before its targeted delivery to intracellular components like DNA or RNA, hence, we investigated the fluorescence property of E-GO complex in presence of HSA also, a major protein component presents in blood. Remarkably, the intensified blue fluorescence of the E-GO-HSA (EGH) complex switched to bluish green upon addition of DNA, thereby directing towards potential use of GO

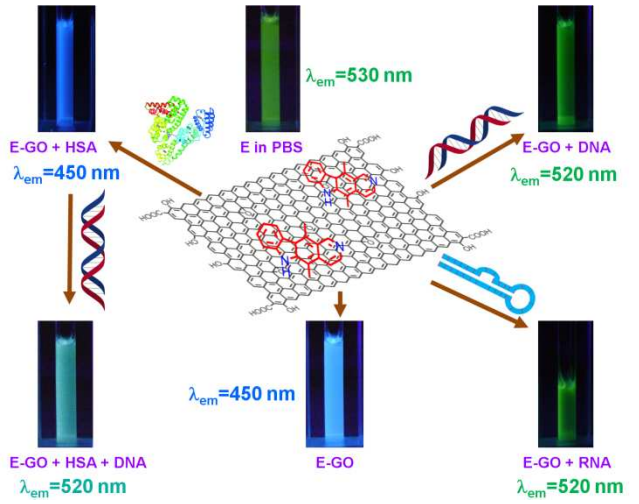

Fig. 1 Fluorescence-switching of ellipticine in presence of GO with various bio-macromolecules (HSA/dsDNA/RNA).

for site-specific delivery of E without much change in pH which sometimes seemed to play a crucial role.[33] However, with addition of sugar to the E-GO complex, no such fluorescence-switching was observed. All the fluorescence-switching experiments are performed in this work are schematically presented in Figure 1. We attribute the observed unique fluorescence-switching originating from the self-assembly of various components as evidenced from the electron microscopy results and mediated by specific interactions with E.

Results and Discussion

Charecterizations of Graphene Oxide (GO)

Results of GO charecterizations are presented in Figure 2. Overall, our results are in good agreements with those reported earlier.[34-36] Specifically, observation of the characteristics (i) stretching vibrations at 1056 cm^{-1} (epoxide or alkoxy -C–O), 1384 cm^{-1} (carboxyl C-O), 1630 cm^{-1} (graphene C=C), 1710 cm^{-1} (carbonyl moiety in –COOH) and 3444 cm^{-1} (-OH) in the FTIR spectrum (Figure 2a); (ii) D and G bands at 1336 cm^{-1} and 1596 cm^{-1} in the Raman spectrum[18, 34] (Figure 2b) altogether confirm the formation of GO. In Raman spectra, compared to graphite, the intensity of the D band (I_D) increases while the intensity of the G band (I_G) decreases (I_D/I_G = 0.34 for graphite and I_D/I_G = 1.10833 for GO (Table S1)) and both the bands are relatively broad in GO. The thermal stability of GO investigated by thermogravimetric analysis (TGA) (Figure 2c), shows weight loss of ~20% below 100 °C and is primarily attributed to the trapped water molecules in between the π-stacked sheets.[35] The further weight loss amounting to ~50% around 200 °C could be due to pyrolysis of labile hydroxyl, epoxy and carboxyl groups.[35] Atomic force microscopy (AFM) image (Figure 2d) exhibits two-dimensional sheets of GO with lateral dimension in the range of tens to hundreds of nanometers and thickness of ~1 nm, which corroborates well with the previous report.[36] Furthermore, HR-TEM image of GO (Figure 2e) clearly supports the AFM observations by showing a layered structure with a single layer resolution.

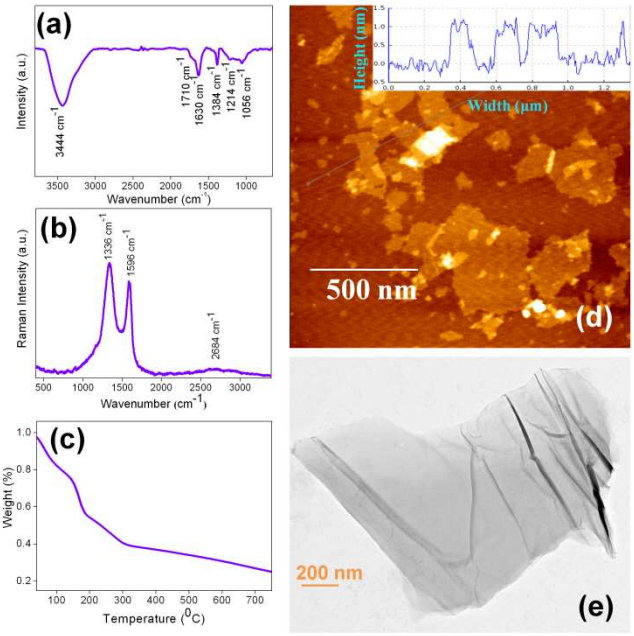

Fig. 2 Graphene oxide characterizations (a) FTIR spectra; (b) Raman spectra; (c) Thermal gravimetric analysis (TGA) curve at heating rate of 10°C/minute in nitrogen; (d) AFM image and depth profile of as prepared single layer GO and (e) HR-TEM image of GO.

Steady State Fluorescence Spectroscopy

Ellipticine (E) in aqueous buffer medium predominantly exists in protonated form (Scheme 1) (as the pK_a of quinoline nitrogen is ~7.4[30]) and shows green emission at 530 nm[30-32] (Figure 3a). With progressive addition of GO, the peak at 530 nm gradually shifts towards lower wavelength and finally emits blue light at 450 nm (Figure 3a). Interestingly, we observe hike in the blue fluorescence intensity with the gradual addition of GO, and this observation differs from the previous findings, where GO acts as energy acceptor and quenches the fluorescence of drugs/fluorophore.[37, 38] Notably, all the prevoius cases where quenching is observed, there is no new species is generated in presence of GO. However, in our case neutral form of E generates at the cost of protonated form at the GO surface. Therefore, this counterintutive fluorescence behavior of E may be attributed to the increased population of neutral ellipticine molecules at the GO surface by the progressive addition of GO to the ellipticine containing buffer solution (Figure S2a, Figure S3 in ESI). Notably, similar kind of fluorescence enhancement was also observed for graphene bound -HPTS (8-hydroxy-1,3,6-pyrenetrisulfonic acid trisodium salt) and -DHPDS (6,8-dihydroxy-1,3-pyrenedisulfonic acid disodium salt), and it was attributed to shift of acid-base equilibrium in presence of graphene.[39] As blue emission corresponds to the neutral form of ellipticine (E_N) (Scheme 1),[30-32] it infers that E_N selectively binds to the GO surface mainly through π-π stacking interaction with a loading capacity of ~76% off its initial concentarion (Note 2 in ESI), indicating GO can be used as a potential carrier for E (detection limit is 1.33 μM/μg of GO).

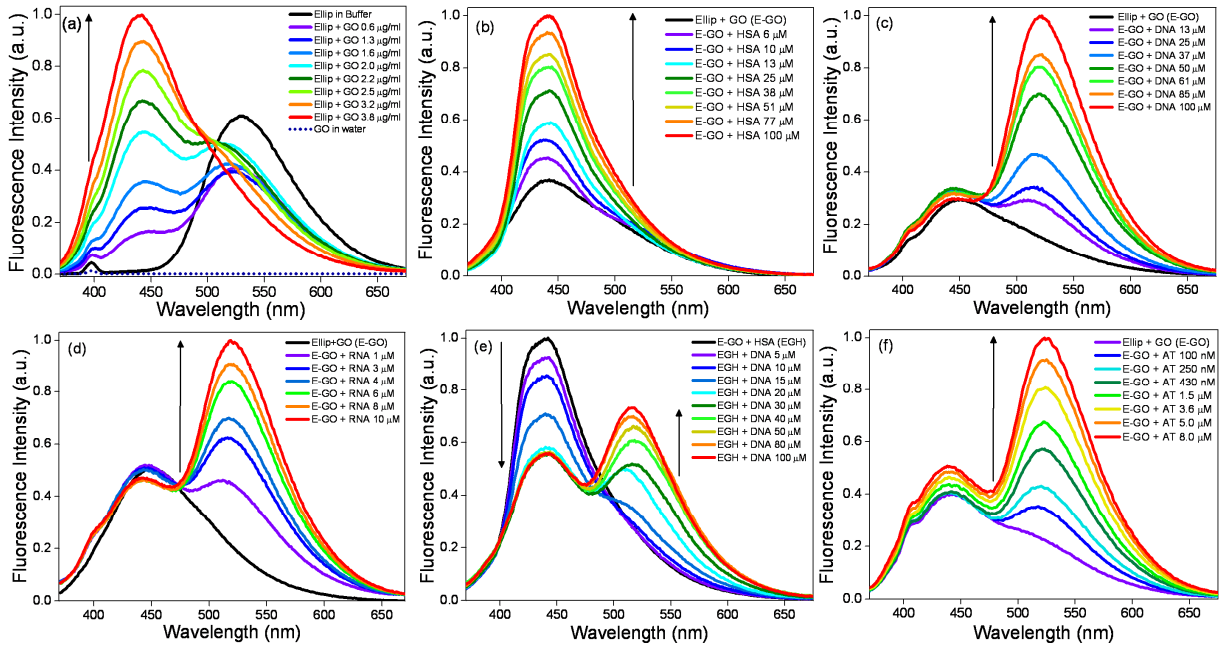

Fig. 3 Fluorescence profiles (λ_{ex}=355 nm) of (a) ellipticine with GO (0-3.8 μg/ml); (b) E-GO with HSA (0-100 μM); (c) E-GO with Salmon sperm DNA (0-100 μM); (d) E-GO with TAR-RNA (0-10 μM); (e) EGH (HSA=100 μM) with Salmon sperm DNA (0-100 μM); (f) E-GO with $(dA\text{-}dT)_{15}$ (0-8 μM). The dotted spectrum in (a) represents the emission profile of GO in buffer at the same experimental conditions.

After that we were curious to know whether the drug interacts with serum albumin protein, which is rich in blood serum. With gradual addition of HSA to the E-GO system (Figure 3b), the blue emission gets intensified, inferring E_N is interacting strongly with protein. Here it is pertinent to mention that E normally binds with protein in its neutral form (E_N) and hence, the intensification of blue emission might arise either from the binding of free E molecules with the protein and/or interaction of GO-bound E_N molecules with the protein. It is already evidenced from the previous reports that protein generally adsorbs on the surface of GO by hydrophobic, π-π stacking interactions with π-conjugated sub-domains, hydrogen bonding interactions (between the oxygen functional groups of GO and nitrogen and oxygen containing functional groups of protein) as well as electrostatic interactions between protein surface charges and oxygen functional groups over GO.[8, 19, 20, 40] Note that in Raman spectrum (Figure 2b), two distinctive bands at 1336 cm^{-1} (D-band) and 1596 cm^{-1} (G-band) are represenative of sp^3 and sp^2 C-atoms, respectively on the GO.

In comparison to graphite (Figure S1e), the observed alteration of intensity ratio between D and G-bands (I_D/I_G) provides information on the structural parameters, specifically the π-cunjugation.[18, 34] The crystalline size in the graphene layers is determined to be L_c= 4.4 (I_G/I_D)[41] (Table S1), which is three times lower than that of graphite. This L_c indicats that few domains of graphitic fraction exists over GO on which ellipticine and biomolecules can also bind via π-π interaction. Therefore, we believe that the enhancement of blue emission of E is an outcome of adsorbed protein on GO surface (in which E_N molecules experiences more hydrophobic environment in presence of protein), and it is supported by circular dichroism (CD) (Note 3 in ESI) and time-resolved spectroscopy results (Note 4, 5 in ESI). In view of drug delivery experiments, this observation has significant implication which assures during the journey through the blood stream ellipticine (E) will not be easily released from the GO surface as it is further protected by serum protein.

As GO has the ability to penetrate the cell,[8] which is enriched with DNA and RNA, next step is to check the interaction behavior of E-GO composite with the above mentioned biopolymers. To execute this experiment, we have taken salmon sperm DNA, $(dA\text{-}dT)_{15}$ and TAR-RNA. In presence of DNA, GO bound E exhibits a new emission peak at 520 nm, in addition to 450 nm peak (Figure 3c, 3f). With the progressive increase of DNA concentration, the peak at 520 nm dominates over 450 nm peak (Figure 3c, 3f). At high DNA concentration, the 520 nm becomes major peak along with a small hump at 450 nm and it reflects a clear fluorescence-switch from blue to green colour (Figure 1). The binding constant (K_f) is estimated to be $(6.18\pm0.6) \times 10^5$ M^{-1} from Scatchard plot (Note 6 in ESI), which is very close to the value obtained from chromatin-DNA bound ellipticine (E)[30]. Almost similar observation is noticed in case of TAR-RNA (Figure 3d) and the binding constant (K_f = $(1.014\pm0.1) \times 10^5$ M^{-1}) estimated from the Scatchard plot (Note 6 in ESI) is lower than that of DNA. Our Raman results (discussed later) also indicate that composite formation of DNA and TAR-RNA with GO exhibits different modulation in the peak intensities of characteristic G and D-bands (I_D/I_G = 1.24 and I_D/I_G = 1.17 for DNA and RNA, respectively), which could be due to slightly different interaction scenario of DNA and TAR-RNA with GO. Here it is pertinent to mention that TAR-RNA (29 bases) consists of bulge, loop and a double stranded (arising from 20 complimentary bases) secondary structure[42] and it is known that protonated form of ellipticine (E_H^+) interacts with DNA/RNA through intercalative mode of binding[43]. Therefore, the lower affinity of ellipticine towards RNA may be attributed to the presence of bulge and loop secondary structures in case of TAR-RNA, which is absent in case of DNA. In our case, the selective

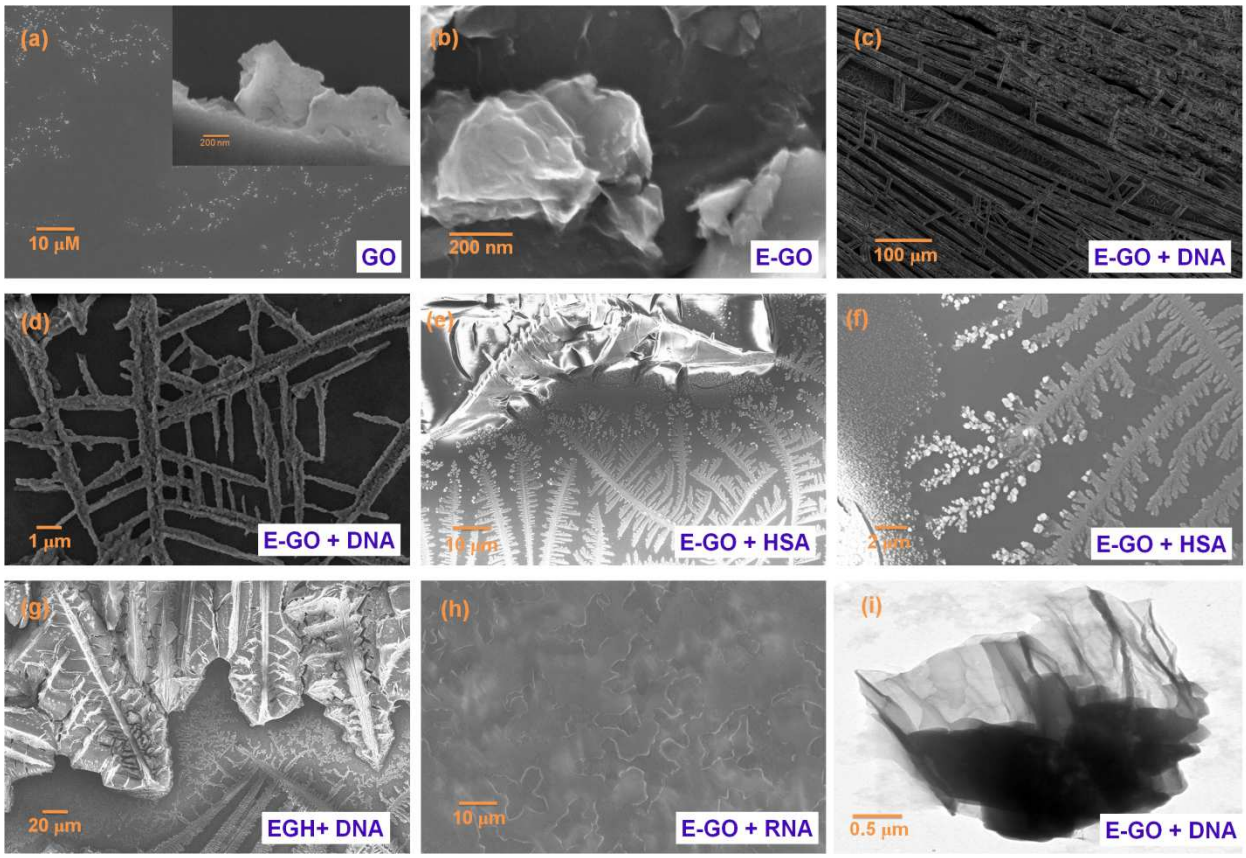

Fig. 4 FE-SEM images of (a) GO (3.8 μg/ml) in aqueous PBS (inset is closed view); (b) ellipticine (7 μM) with GO (3.8 μg/ml) in PBS (E-GO complex); (c) E-GO complex with Salmon sperm DNA (100 μM); (d) closed view of (c); (e) E-GO complex with HSA (100 μM) (E-GO-HSA); (f) closed view of (e); (g) E-GO-HSA with DNA (100 μM); (h) E-GO complex with TAR-RNA (10 μM); (i) HR-TEM image of E-GO complex with Salmon sperm DNA.

detection of RNA/DNA by ellipticine is difficult, as the drug interacts with RNA/DNA with the protonated form, and leads to the enhancement of 520 nm peak in either of the cases. Therefore, unlike other probes,[44] selective detection of DNA/RNA is not possible in the present scenario. The sensitiviy of our system is verified by the experiment with smaller dsDNA ($(dA\text{-}dT)_{15}$), and we found almost ~100 nM (Figure 3f) is able to detect by E-GO system.

The binding affinity of the drug towards DNA/RNA is also supported by steady state anisotropy measurement, where it has been observed that with the gradual addition of DNA, anisotropy value of E rises up and gets saturated at ~40 μM DNA (Note 7 in ESI). As the intensity at 450 nm does not vanish completely, we believe that there are few E molecules, which stick to GO surface, cannot be released even at higher concentration of DNA/RNA. The releasing capacities of GO bound E are 60% and 65% (Note 2 in ESI) for DNA and RNA, respectively. UV-Vis absorption spectra (Figure S2) and fluorescence excitation spectra (Figure S6) further confirms the release of the drug from GO surface in presence of DNA/RNA, as a distinct peak is appeared at ~315 nm, which is attributed to DNA/RNA bound ellipticine molecules[45]. The interaction behavior between E-GO and DNA/RNA are also probed as well as time-resolved measurements in ESI (Note 4, 5 in ESI).

Note that the biological activity of E depends on the intercalation with DNA/RNA.[43] Therefore, it is important to demonstrate the interaction of GO bound E towards DNA/RNA and in order to do so, we have titrated E-GO-HSA (EGH) system with salmon sperm DNA (Figure 3e). It has been observed that DNA extracts E from protein-GO system, which is reflected through the appearance of a new peak at 520 nm in presence of DNA (Figure 3e). The peak at 520 nm becomes dominating at higher DNA concentration and it is reflected by the bluish green fluorescence of the solution. An important finding from this observation is that DNA has better binding affinity than HSA in a competing situation, which is essential for the functioning of ellipticine as a potential anti-cancer drug. To further demonstrate the specificity of E-GO system towards another important bio-molecule, namely, sugar, we have titrated E-GO system with various concentration of glucose (Figure S4). Interestingly, neither increase in intensity likewise HSA nor fluorescence-switching likewise DNA/RNA is observed. Our GO-based molecular switch for sensing important biomolecules resembles GO-based molecular beacon for detection of DNA-binding transcription factor, where GO played the role of a nanoquencher,[46] however, in the present study GO provided the platform of fluorescence switching .

Scanning and Transmission Electron Microscopy Studies

The microstructures of GO, E-GO, EGH, EGH-DNA and E-GO-

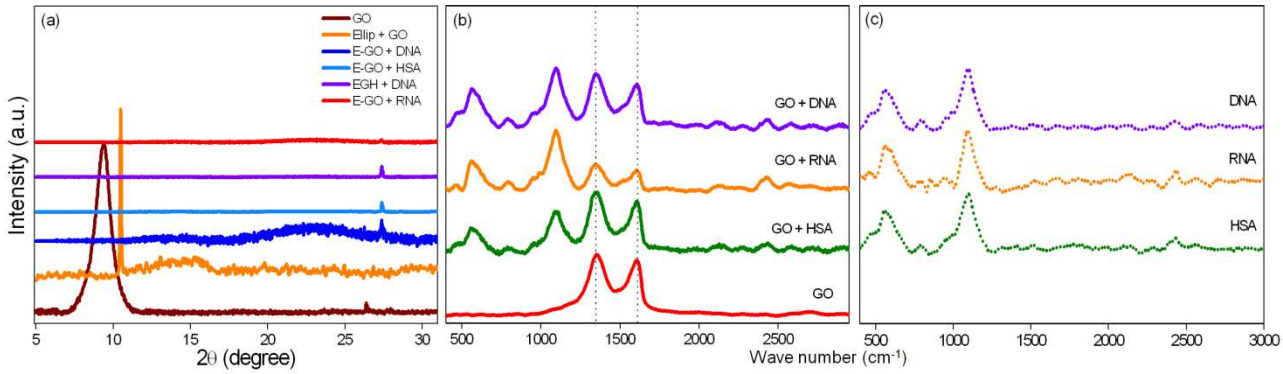

Fig. 5 (a) Powder XRD pattern of GO, E-GO with various biomolecules; (b) Raman spectra of GO, GO with HSA, GO with RNA, GO with salmon sperm DNA; (c) Raman spectra of HSA, RNA and DNA.

DNA/RNA were imaged by FE-SEM. From FE-SEM images, stacked-layers of GO platelets can be identified (Figure 4a), which is consistent with the AFM (Figure 1d) as well as HR-TEM (Figure 1e) observation of isolated GO platelets. Addition of ellipticine (E) apparently did not change the morphology of GO (Figure 4b), which could be due to an easy intercalation of small E molecules in between the layers of GO mainly through π-π stacking interactions (see discussions in earlier section). Since GO has negligible fluorescence compared to E (Figure 3a), the fluorescence-switching from green to blue in presence of GO is attributed to the formation of E_N molecules inside the stacked layer of GO, primarily driving the equilibrium of $E_N \rightleftharpoons E_H^+$ towards the left.

Addition of DNA/RNA to E-GO system dramatically alters the morphology (Figure 4c, 4d, 4h) and this morphology is totally different from ellipticine-DNA/RNA morphology (Figure S1). We believe that π-π stacked E-GO layers were completely exfoliated in presence of DNA/RNA and an extended (hundreds of microns) networks of dsDNA-GO hybrid were formed involving similar interaction likewise the formation of DNA-carbon nanotube hybrids.[47, 48] HR-TEM image (Figure 4i) also supports the FE-SEM observation and at the same time confirms the presence of the both GO and DNA in the GO-DNA hybrid composite likewise previously reported DNA-directed self-assembled structure of GO.[49] Once the exfoliation is achieved by DNA/RNA, E is left in PBS solution with its protonated (E_H^+) form, which can be stabilized by the negative surface charge of DNA/RNA via electrostatic interactions. However, we cannot rule out the possibility that in presence of DNA/RNA, the drug desorbs and binds with DNA/RNA. Either of the case, the blue shift in the fluorescence peak (~530 nm in PBS to ~520 nm in DNA/RNA) reveals the interaction between E_H^+ and DNA/RNA. In case of ellipticine-GO-HSA (EGH) composite (Figure 4e, 4f), the distinctive assembly of HSA into leaf-like fashion is visible and GO platelets are aggregated at the leaf-edges. Interestingly, this kind of assembly structure is absent in case of ellipticine-HSA (Figure S1a). Therefore, this distinctive interaction feature of EGH composite system may be ascribed to the self-assembled structure of GO and HSA.

The observed intensity enhancement in the blue-fluorescence of EGH composite could be due to insertion of additional E_N moieties into the hydrophobic cavities of HSA that overall shifts the equilibrium ($E_N \rightleftharpoons E_H^+$) more towards left. Astonishingly, upon addition of DNA to the EGH composite (Figure 4g), the morphology changes significantly. The aggregated particle like features, (which are visible near leaf-edges of HSA in Figure 4f) no longer exist, rather it is extending into network and also, the leaf-like features of HSA assembly were somewhat modified (Figure 4g). Such edge-assembly of HSA-DNA supports the distinctive ternary complex formation as proposed during DNA-protein interactions study.[29, 50] Overall, the assembly driving the equilibrium towards protonated form of E (E_H^+) and thus switching of fluorescence from blue to bluish green occurred.

Interestingly, the E-GO-RNA composite exhibited entirely different morphology (Figure 4h) in comparison to the E-GO-DNA composite (compare to E-RNA Figure S1c), although the fluorescence features of both the above mentioned composites are same. This could be related to slightly different secondary structure of DNA and RNA, as we have already discussed in the previous section.

Powder X-Ray Diffraction and Raman Spectroscopy

Results from FE-SEM analysis are complemented by PXRD patterns presented in Figure 5a. The characteristic 2θ peak at ~9.36° corresponding to interlayer spacing of ~9.45 Å of GO is modulated upon interaction with E_N moieties (2θ ~10.5°). The reduction of the interlayer spacing to ~8.42 Å suggests an efficient intercalation of E_N predominantly through π-π interaction and thereby E acts as a gluing agent in sticking the GO sheets. Notably, in earlier reports on the 3D self-assembly of GO and ssDNA resulted in the formation of the composite materials for which no characteristics PXRD peak of GO was observed.[51, 52] Similarly, in our composite systems (between GO and HSA/dsDNA/RNA), no such characteristic PXRD peaks of GO was detected and thus infers that complete exfoliation took place in the course of formation of various composite systems due to hydrogen bonding (between polar functional groups of GO and primary amines of DNA[52]), van der Waals force and hydrophobic interactions between of GO and DNA/RNA.[53, 54] To our knowledge, such morphological pattern specifically of GO with dsDNA originating from the three-dimensional self-assembly is very unusual and reported here for the first time. We believe this kind of GO-DNA network structures could find potential application in the fabrication of biomedical devices such

as GO based field effect transistors and bio-cellular devices.[55-57]

Keeping in mind the fact that PXRD is not an ideal tool to conclusively prove or disprove the presence of GO in various composite systems prepared here, we have further carried out Raman spectroscopy and the spectra are shown in Figure 5b and 5c. Characteristic Raman signatures of both GO and different biomolecules can be easily identified in the spectra of various self-assembled composite systems like GO-DNA, GO-RNA, GO-HSA and GO-HSA-DNA.

It is also noteworthy to mention that E-GO, E-GO-DNA, EGH and EGH-DNA systems in PBS solution were stable even at ambient conditions for more than 64 hrs (Note 8 in ESI). Thus, the additional functionalization step of GO which has so far been routinely used in various drug delivery experiments[7-11] is perhaps not necessary.

Conclusions

We have demonstrated here GO-based fluorescence-switching of ellipticine (E), during its loading onto GO and subsequent release to specific biomolecules at physiological pH. Up to 76% of initial concentration of ellipticine (E) can be efficiently loaded onto GO, out of which 60-65% can be released to DNA/RNA but not to glucose. Finally, we have shown that E can also be released to DNA even from the E-GO-HSA composite. Electron microscopy (FE-SEM and HR-TEM), X-ray diffraction and Raman Spectroscopy altogether suggest the formation of distinctive 3D assemblies involving GO and biomolecule(s) probably through non-covalent interactions and responsible for the biomolcule(s) assisted fluorescence-switching of E. Specifically, the GO-DNA assembly seems very unusual and needs further exploration. Here presented fluorescence-switching approach to monitor the drug loading and release through direct optical detection is very cheap and appealing for clinical trial experiments by, keeping the cytotoxicity of GO in minimal range. Moreover, our work is expected to stimulate future experiments across physical chemistry, bio-chemistry, computational chemistry and material science, for the development of various GO-based self-assembled structures with important biomolecules.

Experimental Section

Materials and Instrumentation

Graphite flakes, ellipticine (High purity > 99%), human serum albumin (fatty acid and globulin free, purity ~99%), Salmon's sperm DNA were purchased from Sigma-Aldrich, and were used without any further purification. $(dA\text{-}dT)_{15}$ was purchased from Integrated DNA Technologies (IDT) and was used without any further purification, whereas trans activating responsive RNA (TAR-RNA) (Sequence: 5′-GGC AGA GAG CUC CCA GGC UCA GAU CUG CC-3′) was synthesized by in vitro transcription reaction using TAR-DNA template and T7 promoter. Powder X-ray diffraction (PXRD) spectra of GO were collected using Bruker D8-Advance X-ray powder diffractometer (Cu Kα radiation; λ=1.5418 Å). The field emission scanning electron microscope (FE-SEM) images of GO were obtained from ZEISS, Ultra Plus. High resolution transmission electron microscope (HR-TEM) images were obtained with a Technai-300 transmission electron microscope opened at an accelerating voltage of 200 kV. The samples were drop casted on a Cu grid and left to dry in air for 12 hours. Atomic force microscopy (AFM) characterizations are done by NanoWizard II (JPK instruments, Germany) and Raman spectra were collected using Lab RAM HR 800 (Horiba scientific) 532 nm excitation. Thermogravimetric analysis was done by using STA 6000 from Perkin Elmer. Fourier transform infrared (FTIR) spectrum was performed in NICOLET 6700 FTIR from Thermo Scientific. Circular dichroism (CD) spectra were recorded on a J-815 CD (JASCO, USA). Absorption measurements were performed on EVOLUTION 300 UV-Visible spectrometer (Thermo Scientific) and steady state fluorescence were recorded in Flouromax-4 (HORIBA scientific, USA). All time-resolved fluorescence measurements were taken by a time correlated single photon counting (TCSPC) spectrometer (Horiba Jobin Yvon IBH, U.K.) with an excitation by 375 nm nano-LED. The detailed description of this instrument is given elsewhere.[58, 59]

Preparation of Graphene Oxide (GO)

Graphene oxide (GO) was synthesized from natural graphite by the typical process.[60] Briefly, graphite powder was put into a mixture of concentrated H_2SO_4, $K_2S_2O_8$ and P_2O_5 at 80 ^{0}C on a hotplate about 6 hours. The mixture was cooled to room temperature, diluted with water and left overnight. Then it was washed several times with de-ionized water and pre-oxidized graphite (POG) was obtained. Then POG was subjected to oxidation and obtained GO washed with de-ionized water, followed by aqueous HCl (v/v 10%) and ethanol solution (Details in Note 1 in ESI). Finally, the sample was dried in vacuum oven overnight.

Sample preparation

Concentrated ellipticine (E) stock solution was prepared in DMSO solvent. 4 µl of this stock solution was added into 4 ml of aqueous buffer solution (pH 7) and strongly sonicated to obtain a homogeneous solution in PBS. For all the experiments, the concentration of E was kept ~7×10^{-6} M^{-1}. GO (0.16 mg/ml) stock solution was prepared in aqueous solution by strong sonication about 2 hrs, centrifuged ~14,000 rpm to remove large sized GO sheets and supernant solution was used for titration to the E containing PBS solution. DNA, RNA samples are preoperly annealed at ~95^0 C and gradually allowed to cool at room temperature. Concentration of salmon sperm DNA was estimated by its absorbance at 260 nm using extinction coefficient 13,800 M^{-1} cm^{-1} per base pair.[61] As $(dA\text{-}dT)_{15}$ is small DNA, hence we have estimated concentration by using its cumulative molar extinction coefficient of all bases 3,32,200 M^{-1} cm^{-1} (at 260 nm) generated by IDT SciTools and TAR-RNA concentration was measured by its absorbance at 260 nm with using molar extinction coefficient 2,73,800 M^{-1} cm^{-1} generated by IDT SciTools. The molar extinction coefficient of HSA used for concentration calculation is 36,500 M^{-1} cm^{-1} at 280 nm[62]. All the experiments were performed at room temperature in aqueous buffer.

Acknowledgment

This work is partly supported by Council of Scientific and Industrial Research (CSIR), Government of India, DST-

Nanomission (project number SR/NM/NS-42/2003). RKK thanks to UGC for JRF and AS thanks CSIR for SRF. Authors thank to reviewers for their valuable comments and suggestions. Authors thank to the Director, IISER-Pune for providing excellent experimental facilities. This work is dedicated to Prof. K. N. Ganesh on the occasion of his 60th birthday.

Notes and references

Department of Chemistry, Mendeleev Block, Indian Institution of Science Education and Research (IISER), Pune, Dr. Homi Bhabha road, Pashan, Maharashtra - 411008, India.
Fax: 91-20-2589-9790; Tel: 91-20-2590-8077;
E-mail:p.hazra@iiserpune.ac.in, nballav@iiserpune.ac.in
†Electronic Supplementary Information (ESI) available: Experimental procedure, absorption spectra, in-vitro drug loading, releasing capacity, CD measurements, Raman spectra, time-resolved measurements, Scatchard plots for binding constant, steady state anisotropy and normal images of GO solubility. See DOI: 10.1039/b000000x/

1. J. Siepmann, R. A. Siegel and M. J. Rathbone, Springer, New York, U.S.A., 2012.
2. R. A. Petros and J. M. DeSimone, *Nat. Rev. Drug Discov.*, 2010, **9**, 615-627.
3. K. Cho, X. Wang, S. Nie, Z. Chen and D. M. Shin, *Clin. Cancer Res.*, 2008, **14**, 1310-1316.
4. L. Yuan, Q. Tang, D. Yang, J. Z. Zhang, F. Zhang and J. Hu, *J. Phys. Chem. C*, 2011, **115**, 9926-9932.
5. J. E. Gagner, S. Shrivastava, X. Qian, J. S. Dordick and R. W. Siegel, *J. Phys. Chem. Lett.*, 2012, **3**, 3149-3158.
6. K. S. Novoselov, A. K. Geim, S. V. Morozov, D. Jiang, Y. Zhang, S. V. Dubonos, I. V. Grigorieva and A. A. Firsov, *Science*, 2004, **306**, 666-669.
7. C. Chung, Y.-K. Kim, D. Shin, S.-R. Ryoo, B. H. Hong and D.-H. Min, *Acc. Chem. Res.*, 2013, DOI: 10.1021/ar300159f.
8. H. Y. Mao, S. Laurent, W. Chen, O. Akhavan, M. Imani, A. A. Ashkarran and M. Mahmoudi, *Chem. Rev.*, 2013, **113**, 3407-3424.
9. K. Yang, L. Feng, X. Shi and Z. Liu, *Chem. Soc. Rev.*, 2013, **42**, 530-547.
10. Y. Zhang, T. R. Nayak, H. Hong and W. Cai, *Nanoscale*, 2012, **4**, 3833-3842.
11. Y. Wang, Z. Li, J. Wang, J. Li and Y. Lin, *Trends biotechnol.*, 2011, **29**, 205-212.
12. Y. Pan, N. G. Sahoo and L. Li, *Expert Opin. Drug Del.*, 2012, **9**, 1365-1376.
13. Z. Liu, J. T. Robinson, X. Sun and H. Dai, *J. Am. Chem. Soc.*, 2008, **130**, 10876-10877.
14. G. Wei, M. Yan, R. Dong, D. Wang, X. Zhou, J. Chen and J. Hao, *Chem. Eur. J.*, 2012, **18**, 14708-14716.
15. J. W. Yi, J. Park, N. J. Singh, I. J. Lee, K. S. Kim and B. H. Kim, *Bioorg. Med. Chem. Lett.*, 2011, **21**, 704-706.
16. J. Balapanuru, J.-X. Yang, S. Xiao, Q. Bao, M. Jahan, L. Polavarapu, J. Wei, Q.-H. Xu and K. P. Loh, *Angew. Chem. Int. Ed.*, 2010, **49**, 6549-6553.
17. J. W. Yi, J. Park, K. S. Kim and B. H. Kim, *Org. Biomol. Chem.*, 2011, **9**, 7434-7438.
18. K. Liu, J.-J. Zhang, F.-F. Cheng, T.-T. Zheng, C. Wang and J.-J. Zhu, *J. Mater. Chem.*, 2011, **21**, 12034-12040.
19. F. Yang, Y. Liu, L. Gao and J. Sun, *J. Phys. Chem. C*, 2010, **114**, 22085-22091.
20. J. Liu, S. Fu, B. Yuan, Y. Li and Z. Deng, *J. Am. Chem. Soc.*, 2010, **132**, 7279-7281.
21. W. Hu, C. Peng, M. Lv, X. Li, Y. Zhang, N. Chen, C. Fan and Q. Huang, *ACS Nano*, 2011, **5**, 3693-3700.
22. E. L. K. Chng and M. Pumera, *Chem. Eur. J.*, 2013, **19**, 8227-8235.
23. H. Bao, Y. Pan, Y. Ping, N. G. Sahoo, T. Wu, L. Li, J. Li and L. H. Gan, *Small*, 2011, **7**, 1569-1578.
24. Y. Pan, H. Bao, N. G. Sahoo, T. Wu and L. Li, *Adv. Func. Mater.*, 2011, **21**, 2754-2763.
25. G. Xin, H. Wang, N. Kim, W. Hwang, S. M. Cho and H. Chae, *Nanoscale*, 2012, **4**, 405-407.
26. J.-B. Le Pecq, Nguyen-Dat-Xuong, C. Gosse and C. Paoletti, *Proc. Natl. Acad. Sci. U.S.A.*, 1974, **71**, 5078-5082.
27. M. Stiborová, C. A. Bieler, M. Wiessler and E. Frei, *Biochem. Pharmacol.*, 2001, **62**, 1675-1684.
28. C. L. Arteaga, D. L. Kisner, A. Goodman and D. D. Von Hoff, *Eur. J. Cancer Clin. On.*, 1987, **23**, 1621-1626.
29. S. J. Froelich-Ammon, M. W. Patchan, N. Osheroff and R. B. Thompson, *J. Biol. Chem.*, 1995, **270**, 14998-15004.
30. F. Sureau, F. Moreau, J. M. Millot, M. Manfait, B. Allard, J. Aubard and M. A. Schwaller, *Biophys. J.*, 1993, **65**, 1767-1774.
31. S. Y. Fung, J. Duhamel and P. Chen, *J. Phys. Chem. A*, 2006, **110**, 11446-11454.
32. Z. Miskolczy, L. Biczók and I. Jablonkai, *Chem. Phys. Lett.*, 2006, **427**, 76-81.
33. T. Kavitha, S. I. Haider Abdi and S.-Y. Park, *Phys. Chem. Chem. Phys.*, 2013, **15**, 5176-5185.
34. K. N. Kudin, B. Ozbas, H. C. Schniepp, R. K. Prud'homme, I. A. Aksay and R. Car, *Nano Lett.*, 2007, **8**, 36-41.
35. J. Shen, Y. Hu, C. Li, C. Qin and M. Ye, *Small*, 2009, **5**, 82-85.
36. W. Hu, C. Peng, W. Luo, M. Lv, X. Li, D. Li, Q. Huang and C. Fan, *ACS Nano*, 2010, **4**, 4317-4323.
37. K. P. Loh, Q. Bao, G. Eda and M. Chhowalla, *Nat Chem*, 2010, **2**, 1015-1024.
38. M. Zhang, H.-N. Le and B.-C. Ye, *ACS Appl. Mater. Interfaces*, 2013, **5**, 8278-8282.
39. X. Pan, H. Li, K. T. Nguyen, G. Grüner and Y. Zhao, *J. Phys. Chem. C*, 2012, **116**, 4175-4181.
40. V. Georgakilas, M. Otyepka, A. B. Bourlinos, V. Chandra, N. Kim, K. C. Kemp, P. Hobza, R. Zboril and K. S. Kim, *Chem. Rev.*, 2012, **112**, 6156-6214.
41. T. Gokus, R. R. Nair, A. Bonetti, M. Bőhmler, A. Lombardo, K. S. Novoselov, A. K. Geim, A. C. Ferrari and A. Hartschuh, *ACS Nano*, 2009, **3**, 3963-3968.
42. S. G. Srivatsan and Y. Tor, *Tetrahedron*, 2007, **63**, 3601-3607.
43. W. D. Wilson, L. Ratmeyer, M. Zhao, L. Strekowski and D. Boykin, *Biochemistry*, 1993, **32**, 4098-4104.
44. B. Shirinfar, N. Ahmed, Y. S. Park, G.-S. Cho, I. S. Youn, J.-K. Han, H. G. Nam and K. S. Kim, *J. Am. Chem. Soc.*, 2012, **135**, 90-93.
45. G. Dodin, M.-A. Schwaller, J. Aubard and C. Paoletti, *Eur. J. Biochem.*, 1988, **176**, 371-376.
46. J.-J. Liu, X.-R. Song, Y.-W. Wang, G.-N. Chen and H.-H. Yang, *Nanoscale*, 2012, **4**, 3655-3659.
47. E. N. Primo, P. Cañete-Rosales, S. Bollo, M. D. Rubianes and G. A. Rivas, *Colloids Surf. B.*, 2013, **108**, 329-336.
48. M. Zheng, A. Jagota, M. S. Strano, A. P. Santos, P. Barone, S. G. Chou, B. A. Diner, M. S. Dresselhaus, R. S. McLean, G. B. Onoa, G. G. Samsonidze, E. D. Semke, M. Usrey and D. J. Walls, *Science*, 2003, **302**, 1545-1548.
49. L. Tang, Y. Wang, Y. Liu and J. Li, *ACS Nano*, 2011, **5**, 3817-3822.
50. H. Haruki, B. Gyurcsik, M. Okuwaki and K. Nagata, *FEBS Lett.*, 2003, **555**, 521-527.
51. Y. Xu, Q. Wu, Y. Sun, H. Bai and G. Shi, *ACS Nano*, 2010, **4**, 7358-7362.
52. A. J. Patil, J. L. Vickery, T. B. Scott and S. Mann, *Adv. Mater.*, 2009, **21**, 3159-3164.
53. M. Wu, R. Kempaiah, P.-J. J. Huang, V. Maheshwari and J. Liu, *Langmuir*, 2011, **27**, 2731-2738.
54. V. Kotikam, M. Fernandes and V. A. Kumar, *Phys. Chem. Chem. Phys.*, 2012, **14**, 15003-15006.
55. P. Nguyen and V. Berry, *J. Phys. Chem. Lett.*, 2012, **3**, 1024-1029.
56. Q. He, H. G. Sudibya, Z. Yin, S. Wu, H. Li, F. Boey, W. Huang, P. Chen and H. Zhang, *ACS Nano*, 2010, **4**, 3201-3208.
57. T. Cohen-Karni, Q. Qing, Q. Li, Y. Fang and C. M. Lieber, *Nano Lett.*, 2010, **10**, 1098-1102.
58. K. Gavvala, A. Sengupta and P. Hazra, *ChemPhysChem*, 2013, **14**, 532-542.
59. K. Gavvala, W. D. Sasikala, A. Sengupta, S. A. Dalvi, A. Mukherjee and P. Hazra, *Phys. Chem. Chem. Phys.*, 2013, **15**, 330-340.

60. N. I. Kovtyukhova, P. J. Ollivier, B. R. Martin, T. E. Mallouk, S. A. Chizhik, E. V. Buzaneva and A. D. Gorchinskiy, *Chem. Mater.*, 1999, **11**, 771-778.
61. J. Völker, H. H. Klump and K. J. Breslauer, *Proc. Natl. Acad. Sci. U.S.A.*, 2001, **98**, 7694-7699.
62. E. Froehlich, J. S. Mandeville, C. J. Jennings, R. Sedaghat-Herati and H. A. Tajmir-Riahi, *J. Phys. Chem. B*, 2009, **113**, 6986-6993.

Graphic Figure

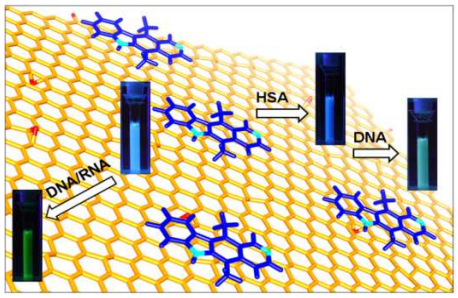

Sensing of Bio-molecules Using Fluorescence-Switch: Dual fluorescence property of an eminent anticancer drug, ellipticine, has been explored to directly monitor its efficient loading onto graphene oxide and subsequent release to biomolecules like DNA/RNA. We propose the observed fluorescence-switching to the unusual three-dimensional self-assembly of graphene oxide with various biomolecules.

Table of Content Entry

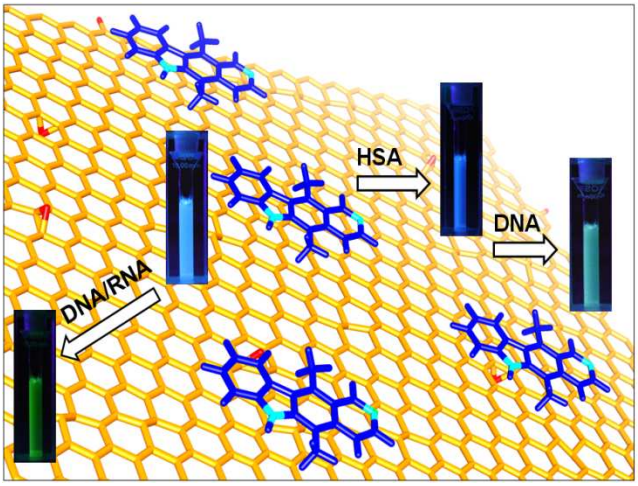

Sensing of Bio-molecules Using Fluorescence-Switch: Dual fluorescence property of an eminent anticancer drug, ellipticine, has been explored to directly monitor its efficient loading onto graphene oxide and subsequent release to biomolecules like DNA/RNA. We propose the observed fluorescence-switching to the unusual three-dimensional self-assembly of graphene oxide with various biomolecules.